

Applications of Nonlinear Magneto-Optic Effects with Ultra-Narrow Widths

Valeriy Yashchuk^{a,b}, Dmitry Budker^{a,c}, and Max Zolotarev^c

^a Department of Physics, University of California, Berkeley, California 94720-7300

^b B. P. Konstantinov Petersburg Nuclear Physics Institute, Gatchina, Russia 188350

^c E. O. Lawrence Berkeley National Laboratory, Berkeley, California 94720

Abstract. A three-axis magnetometer based on the nonlinear magneto-optic effect is described. The magnetometer was used to measure the average (over the cell volume) residual magnetic field and to determine the shielding ratio of a multi-layer magnetic shield. The shot-noise-limited sensitivity of the magnetometer is estimated to be $\approx 10^{-11} \text{ Gs/Hz}^{1/2}$. A possible application to parity and time reversal invariance violation experiments is also considered.

INTRODUCTION

In this paper we discuss applications of the recently observed nonlinear (in light power) magneto-optic effects (NMOE) with effective resonance width $\gamma = g\mu\Delta B_z \approx 2\pi \cdot 1 \text{ Hz}$ (1). Here g is the Lande factor, μ is the Bohr magneton, and ΔB_z is the peak-to-peak width of the dispersion-like magnetic field dependence of NMOE. The small value of γ corresponds to an enhancement of small-field optical rotation ($\varphi_s \propto g\mu B_z / \gamma$), making it useful in low-magnetic field measurements.

NMOE related to the interaction of near-resonant light with atomic vapor in the presence of a magnetic field have been the subject of a number of recent investigations reviewed in (2). Most of the work (see e.g. (3,4,5,6,7)) addresses NMOE in the case of linearly-polarized light propagating along the magnetic field known as nonlinear Faraday rotation. The schematic of an experiment to observe this effect shown in Figure 1 is similar to that of M. Faraday (8), in which he discovered the linear magneto-optical rotation (with non-resonant light), named after him as the Faraday effect. In the experiment, one observes rotation of the linear polarization plane of light as it passes through a medium exposed to a longitudinal magnetic field. In our case, the medium is Rb vapor contained in a paraffin-coated cell with no buffer gas. The light frequency dependence of magneto-optic rotation in the vicinity of a resonance absorption line has a characteristic resonant profile (the Macaluso-Corbino effect (9)). In a complementary picture, the magnetic field dependence of the Faraday effect with a fixed light frequency, one observes several nested dispersion-like features with vastly different widths. This is illustrated in Figure 2 (1). The feature represented in Figure 2 by the overall slope and reaching a maximum at several Gauss is due to hole burning in the velocity distribution of ground state atoms induced by velocity selective optical pumping. The Faraday rotation with such velocity distribution can be thought of as rotation produced by the Maxwell-distributed atoms without the hole (with the Macaluso-Corbino spectral profile) *minus* the rotation that would have been produced by the pumped out atoms. While the effective width of the Macaluso-Corbino effect corresponds to the Doppler-broadened line width (300 MHz), the hole burning effect has effective width $\sim 6 \text{ MHz}$ determined by the natural width of the excited state. Significantly narrower features arise due to long-lived light-induced alignment of the atomic ground state (10) resulting from the process known as coherent population trapping (11). An ensemble of aligned atoms constitutes a medium with linear dichroism. In the presence of a magnetic field, the dichroism axis precesses around the direction of the field with the Larmor frequency. The effect of this precession on the light polarization can be understood if one thinks of the atomic medium as a layer of dichroic polarizing material rotating in the magnetic field, see e. g. (5,1). According to this picture, the effective width γ is determined by the alignment relaxation rate. For sufficiently low light power, this model allows one to achieve quantitative description of dispersion-like shaped Faraday rotation due to the coherence effect as well as of the characteristic behavior of nonlinear optical rotation in the presence of transverse magnetic fields (1,12,13). In Figure 2, the coherence effect is represented by two dispersion-like features corresponding to different processes leading to the relaxation of the ground state alignment. The $\Delta B_z \approx 120 \text{ mGs}$ width of the broader structure is determined by the atoms' transit time through the laser beam. The aligned atoms fly out of the laser beam, while "fresh" atoms from the volume of the cell replace them. This effectively provides for the alignment relaxation. The inserts in Figure 2 show the narrowest NMOE features observed so far (1). Their effective

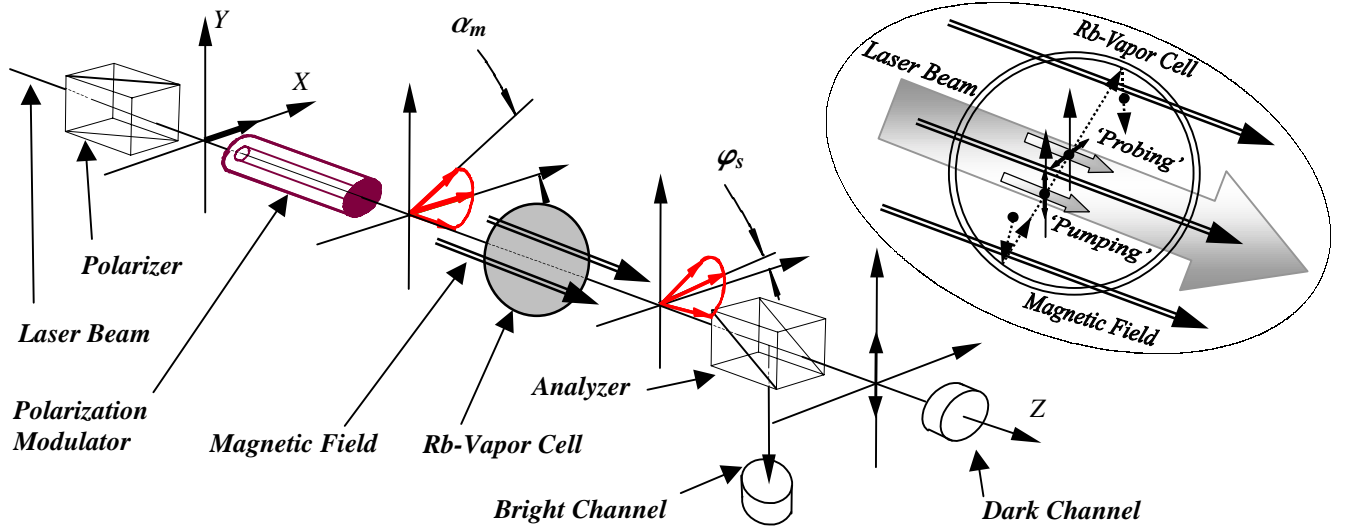


FIGURE 1. Schematic of an experiment to observe NMOE with Rb vapor. The Rb atoms aligned by linearly polarized light represent a magneto-optically active medium in a magnetic field. The measure of the polarization rotation angle is the intensity of light passing through the analyzer crossed with the polarizer. The details of the modulation polarimeter are described in the text. The inset illustrates the mechanisms for the coherence effect.

width is $\gamma = g\mu\Delta B_z/\hbar \approx 2\pi \cdot 1.3 \text{ Hz}$, where $\Delta B_z \approx 2.8 \mu\text{Gs}$. The width is determined by spin-exchange collisions among Rb atoms in the cell. The corresponding relaxation time, 250 ms, shows that the alignment is preserved over several thousand wall-collisions.

In this paper, we consider an application of nonlinear magneto-optic effects with ultra-narrow ($\sim 1 \text{ Hz}$) widths for three-axis magnetometry. The sensitivity of a possible experiment to search for a parity (P) and time reversal invariance (T) violating electric dipole moment (EDM) in cesium is also estimated based on the sensitivity to the magnetic field.

THE LOW-FIELD MAGNETOMETER

The experimental set-up was described in (1). It incorporates a paraffin-coated cell with ^{85}Rb -vapor at room temperature and a modulation polarimeter - Figure 1. The cell (diameter $d=10 \text{ cm}$) has high quality paraffin coating (14), ensuring negligible relaxation of alignment in wall collisions compared to spin-exchange relaxation (1). The cell was surrounded with three mutually perpendicular (3-D) magnetic coils. The coils allow compensation of the residual magnetic field and application of an arbitrarily directed well-controlled field to the cell. An external cavity diode laser is used. In the following we describe experimental results and estimate the magnetometer sensitivity for the $F_g=3 \rightarrow F_e=2,3,4$ transition of the D_2 ($^2S_{1/2} \rightarrow ^2P_{3/2}$; $\lambda=780.2 \text{ nm}$) resonance line of ^{85}Rb . The optical thickness of the vapor at a temperature of 20.5°C was measured to be $d/l_0 \approx 1.4$ for the center of the absorption line. Here l_0 is the unsaturated absorption length. The modulation polarimeter (see Figure 1) incorporates a crossed Glan prism polarizer and a polarizing beam splitter used as an analyzer (extinction ratio $\varepsilon < 5 \cdot 10^{-5}$). A Faraday glass element modulates the direction of the linear polarization of the light at a frequency $\omega_m \approx 2\pi \cdot 1 \text{ kHz}$ with an amplitude $\alpha_m \approx 5 \cdot 10^{-3} \text{ rad}$. The first harmonic of the signal is detected with a lock-in amplifier. Its amplitude, normalized to the transmitted light intensity detected in the bright channel of the analyzer, is a measure of the magneto-optical rotation in the vapor cell, φ_s .

In a magnetometric measurement using this technique, we record the dependences of φ_s on longitudinal magnetic field B_z , scanning an appropriate current in the 3-D coils. Depending on the value of measured field, one of the nested dispersive features, like those shown in Figure 2, is observed. The feature shape and horizontal offset depend strongly on the value and direction of the magnetic field being measured. Fitting a series of experimental curves at different bias currents in the magnetic coils with the model developed in (1) and briefly described in the Introduction we determine all three Cartesian components of magnetic field. The highest sensitivity of the magnetometer is achieved by realizing the effect of alignment preservation in collisions of Rb atoms with paraffin-coated cell walls. To observe this effect, the cell surrounded with 3-D coils is placed inside a four-layer magnetic shield, shown in Figure 3. The shield was manufactured from 0.040" thick CONETIC-AA sheets. The three outer layers of the shield are cylinders with conical lids, while the innermost layer is a cube with rounded edges. The nearly spherical shape of the three outer layers is intended to provide nearly isotropic shielding of an external DC field. Indeed, the shielding ratio for multi-layer shield depends strongly on the shield shape as well as on the

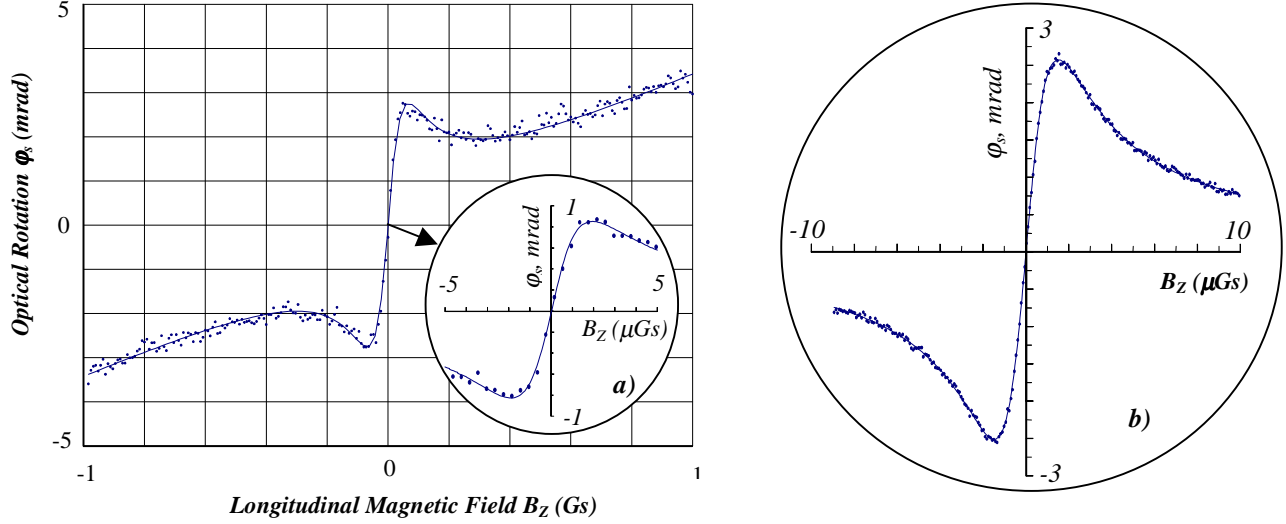


FIGURE 2. Optical rotation dependence on the longitudinal magnetic field (1). **a** - a detailed scan of the near-zero B_Z -field region at a $2 \cdot 10^5 \times$ magnification of the horizontal scale. The experiments were performed with laser tuned on the center of Doppler profile of $F_g = 3 \rightarrow F_e = 2, 3, 4$ transition of ^{85}Rb D_2 resonance line. Light intensity: $W_p \approx 100 \mu\text{W}/\text{cm}$. **b** - a near-zero B_Z -field scan with laser tuned $\approx 460 \text{ MHz}$ towards high frequencies from the line-center. $W_p \approx 520 \mu\text{W}/\text{cm}$.

magnetic field orientation with respect to the shield. It can be estimated as (see, e. g. (15,16)):

$$S_{tot} \equiv \frac{B_{in}}{B_0} \approx S_n \cdot \prod_{i=1}^{n-1} S_i \left(1 - \left(\frac{X_{i+1}}{X_i} \right)^k \right)^{-1}; \quad S_i \approx \frac{X_i}{\mu_i \cdot t_i}. \quad (1)$$

In equations (1), B_0 is the homogeneous magnetic field before introducing the shield, B_{in} is the field inside the shield due to B_0 ; S_i is the shielding factor of a separate i -th layer; X_i are the layer's radius or length (depending on the relative orientation of the magnetic field and the layer); we assume $X_i > X_{i+1}$; t_i and μ_i are the thickness and magnetic permeabilities; n is the number of layers. For estimates, good approximations of the power k are: $k=3$ for a spherical shield; $k=2$ and $k=1$ for the transverse and axial shielding factors of a cylindrical shield with flat lids, respectively. Therefore spherical shells are preferable providing the best shielding properties (for shields of comparable dimensions). In the design of the three outer layers of our shield, we found a compromise between trying to approximate a spherical shape and retaining relative simplicity of manufacturing. The innermost shield has cubic shape (with rounded edges). This allows application of relatively homogeneous fields with a simple system of nested 3-D coils.

As a first application of the described magnetometer, we measured the residual magnetic fields and shielding factors of the shield. The typical components of the residual magnetic field averaged over the volume of the vapor cell were found to be $B_x \approx 53 \mu\text{Gs}$, $B_y \approx 14 \mu\text{Gs}$, and $B_z \approx 6 \mu\text{Gs}$. (These values change after each reassembly of the shield.) The residual magnetic field at the cell is mostly attributed to the residual magnetization of the innermost-shielding layer. The inhomogeneity of this magnetic field is one of possible mechanisms decreasing the relaxation time of atomic alignment. However, in the present experiment it is less important than spin-exchange relaxation (1). In order to reach the highest sensitivity of the magnetometer, the transverse magnetic fields should be compensated to a level corresponding to a small fraction of the observed widths ΔB_Z . Zeroing of transverse magnetic fields is accomplished by finding such currents in the 3-D magnetic coils, for which the observed B_Z -dependence of NMOE has symmetric dispersive shape with minimal effective relaxation width. (This was found to be $\gamma = g\mu\Delta B_Z/\hbar \approx 2\pi \cdot 1.3 \text{ Hz}$, where $g=1/3$ for the $F_g=3$ state.) The zeroed magnetometer was used to measure shielding ratio for a dc magnetic field produced by a set of six magnetic coils surrounding the shield. Unfortunately, due to the space limit, the set (the coils' diameters and separations are nearly the same, $\approx 30''$) is not able to produce a homogeneous field on the shield dimensions. Therefore, estimating the shielding ratio, we took the field produced by the set at the cell location without the shield, as B_0 field. It was found to be $\approx 1 \cdot 10^{-6}$, being approximately independent of field direction. The sensitivity δB_Z of the magnetometer to a magnetic field B_Z can be expressed as:

$$\delta B_Z = \left(\frac{\partial \varphi_s}{\partial B_Z} \right)_{B_Z=0}^{-1} \cdot \delta \varphi_s. \quad (2)$$

The first factor represents the slope of the dependence of the rotation angle φ_s on the magnetic field. It is known from the experiment. The second factor is the sensitivity of the polarimeter to φ_s . We can estimate it for shot-noise limited detection using the parameters of the current set-up. In order to perform this estimation, let us consider an expression for the counting

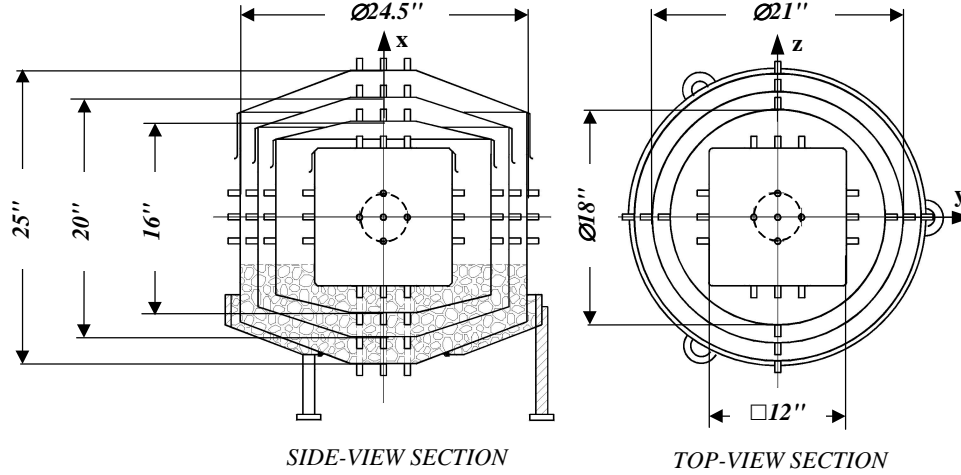


FIGURE 3. Geometrical configuration of the four-layer magnetic shield. The layers are spaced with polyurethane foam to reduce mechanical stress. All CONETIC parts were annealed in a hydrogen atmosphere upon manufacturing. No degaussing was used in the investigations described here. The cell position is shown by dashed-line circle in the center. The shield is designed to allow optical access through a number of 1/2" diameter holes. Each of the holes has an associated 1" stem preserving the shielding properties.

rate from the photodiode placed in the dark channel of the analyzer:

$$N(t) \cong \chi I_p (\varepsilon + \frac{1}{2} \alpha_m^2 + \varphi_s^2) + 2\chi I_p \alpha_m \varphi_s \sin(\omega_m t) - \frac{1}{2} \chi I_p \alpha_m^2 \cos(2\omega_m t). \quad (3)$$

Here χ is the coefficient defined by the absorption and scattering of light by the atomic vapor cell, $\chi \approx 0.2$; I_p is the intensity of linearly polarized light (in photons/sec) transmitted by the polarizer. From the expression (3), for shot-noise-limited detection of the first harmonic signal in the case of an "ideal polarimeter" ($\alpha_m^2 \gg \varepsilon + \varphi_s^2$), one obtains a relation describing the experimental sensitivity of the polarimeter with data accumulation time T :

$$\delta\varphi_s \approx \frac{1}{2 \cdot \sqrt{\chi I_p T}}. \quad (4)$$

As it was found in (1), the light broadening effect is considerably reduced (without attenuating the light power) by working on the slope of the resonance line rather than on the line center, see Figure 2 b). This allows to improve the statistics of the measurement due to increasing both the light intensity and the slope of the magnetic field dependence of φ_s . Therefore, with pumping light intensity $W_p = 520 \mu W/cm^2$ (pumping light cross-section area $S_p = 0.1 cm^2$) one finds:

$$\frac{\partial \varphi_s}{\partial B_z} \cong 3.3 \cdot 10^3 \text{ rad/Gs} \quad \text{and} \quad \delta\varphi_s \approx 3 \cdot 10^{-8} \text{ rad/Hz}^{1/2}, \quad (5)$$

and, consequently, the achievable shot-noise-limited sensitivity δB_z is

$$\delta B_z \approx 10^{-11} \text{ Gs/Hz}^{1/2}. \quad (6)$$

This sensitivity is comparable to or surpasses the best devices based on other techniques. A more detailed comparison to other magnetometers will be given elsewhere.

SENSITIVITY OF A POSSIBLE EDM SEARCH

Application of NMOE in the search for P- and T- violating permanent electric dipole moment (EDM) was first suggested in (17), and later discussed in (6,18). The sketch of a possible EDM experiment is, in general, very similar to the one used to observe the NMOE dependence on B_z . The only principal difference consists in the detection of alignment precession caused by interaction of atom's P- and T- violating EDM d_A with applied electric field E . The shot-noise-limited sensitivity δd_A to the measurement of EDM d_A may be found from the smallest detectable change of the magnetic field, δB_z , according to the relation:

$$\delta d_A = g_J \mu \delta B_z / E, \quad (7)$$

here $g_J = 2$. With the sensitivity δB_z given by expression (6), one obtains:

$$\delta d_{Cs} \approx 10^{-26} \text{ e}\cdot\text{cm}, \quad (8)$$

assuming electric field $E=10\text{ kV/cm}$ and data accumulation time $T=10^6\text{ sec}$. This corresponds to a sensitivity to the electron's EDM, d_e that is, according to theory (see, e.g. (19) and references therein) approximately 120 times smaller:

$$\delta d_e \approx 10^{-28}\text{ e}\cdot\text{cm}. \quad (9)$$

To obtain an EDM limit at the level of statistical sensitivity (9), one has to control possible systematic effects at least at a similar level. We are considering an experiment with a coated cell containing vapors of both Cs and Rb atoms. While the EDM measurements are performed on Cs atoms, Rb will be used as a "co-magnetometer."

CONCLUSIONS

In conclusion, we have considered some applications of NMOE with ultra-narrow widths observed recently in experiments with a ^{85}Rb -vapor cell with a high quality anti-relaxation coating (1). A three-axis magnetometer based on the strong dependence of NMOE on the longitudinal and transverse magnetic fields was developed. The magnetometer was used to determine the shielding ratio of a four-layer magnetic shield shaped to be close to a sphere but retaining relative simplicity of manufacturing. It was found to be $\approx 10^{-6}$ for shielding of an external dc magnetic field in accord with design expectation. The magnetometer was also used to measure and compensate the average (over the cell volume) residual magnetic field. This provided near-zero transverse magnetic field condition at the cell, which was found to be very important in order to achieve the ultra-narrow NMOE features. It was shown that the shot-noise-limited sensitivity of the magnetometer 10^{-11} Gs (for 1-sec data accumulation time) is achieved using the advantages of tuning the laser to the line-slope. Possible application of NMOE in searching for P- and T- violating EDM in atoms has been considered also. We estimated the shot-noise-limited sensitivity of EDM experiment with cesium based on the sensitivity to magnetic field achievable with our set-up. Assuming that it is possible to apply a 10 kV/cm electric field to a paraffin coated cell, this provides statistical sensitivity of $\delta d_{Cs} \sim 10^{-26}\text{ e}\cdot\text{cm}$ and $\delta d_e \sim 10^{-28}\text{ e}\cdot\text{cm}$ for data accumulation time 10^6 sec . These are more than two orders of magnitude better than the current limit for d_{Cs} (20) and about 40 times better than the best published experimental limit on electron EDM, $|d_e| \leq 4 \cdot 10^{-27}\text{ e}\cdot\text{cm}$, established in an experiment with ^{205}Tl (21), respectively.

In the nearest future, we plan to investigate application of high voltage electric fields to a paraffin-coated cell, and the effects of the spin-exchange collisions between rubidium and cesium in the cell in the proposed EDM experiment.

We are grateful to L. R. Hunter for useful comments. This research is supported by ONR, grant # N00014-97-1-0214.

REFERENCES

1. Budker, D., Yashchuk, V., and Zolotarev, M., *Preprint LBNL-42066*, 1998, submitted for publication.
2. Gawlik, W., in: *Modern Nonlinear Optics*, Edited by M. Evans and S. Kielich, New York: Wiley, 1994, Part 3, pp.733-773.
3. Barkov, L. M., Melik-Pashayev, D., and Zolotarev, M., *Opt. Commun.* **70**(6), 467-472 (1989).
4. Zetie, K. P., Warrington, R. B., MacPherson, M. J. D., Stacey, D. N., and Schuller, F., *Opt. Commun.* **91**(3-4), 210-214, (1992).
5. Weis, A., Wurster, J., and Kanorsky, S. I., *J. Opt. Soc. Am. B* **10**(4), 716-724 (1993).
6. Schuh, B., Kanorsky, S. I., Weis, A., and Hänsch, T. W., *Opt. Commun.* **100**(5-6), 451-455, (1993).
7. Kanorsky, S. I., Weis, A., and Skalla, J., *Appl. Phys. B-Lasers and Optics* **60**(2-3), S165-S168 (1995).
8. Faraday, M., *Experimental Research*, **III**, 2164, London, 1855.
9. Macaluso, D., e Corbino, O. M., *Nuovo Cimento* **8**, 257 (1898); *Ibid.* **9**, 384-389 (1899).
10. We use the convention of Alexandrov, E. B., Chaika, M. P., and Kvostenko, G. I., *Interference of Atomic States*, Berlin, Heidelberg, New York: Springer-Verlag, 1993, in which alignment designates the second (quadrupole) polarization moment.
11. Arimondo, E., in *Progress in Optics*, Edited by E. Wolf, Amsterdam: Elsevier, 1996, Vol. 35, pp. 257-354; Brandt, S., Nagel, A., Wynands, R., and Maschede, D., *Phys. Rev. A* **56**(2), R1063-R1066 (1997).
12. Budker, D., Yashchuk, V., and Zolotarev, M., "Study of resonant magneto-optical rotation in the presence of arbitrarily-directed magnetic field," Abstracts of contributed papers, ICAP XVI, Windsor, Canada, August 3-7, 1998, pp. 356-357.
13. Budker, D., Yashchuk, V., and Zolotarev, M., *Preprint LBNL-41149*, 1997, to be published in *Sib. J. Phys.*, 1998.
14. Alexandrov, E. B., Balabas, M. V., Pasgalev, A. S., Vershovskii, A. K., and Yakobson, N. N., *Laser Physics* **6**(2), 244-251 (1996).
15. T. Rikitake. *Magnetic and Electromagnetic Shielding*. Tokyo: TERRAPUB, 1987.
16. Summer, T. J., Pendlebury, J. M., Smith, K.F., *J. Phys. D* **20**(9), 1095-1101 (1987).
17. Barkov, L. M., Zolotarev, M. S., and Melik-Pashayev, D., *JETP Letters* **48**(3), 144-147 (1988). The idea of using optical rotation in longitudinal electric field was suggested in (Sushkov, O. P., Flambaum, V. V., *Zh. Eksp. Teor. Fiz.* **75**(4), 1208-1213 (1978)).
18. Hunter, L. R., *Science* **252**, 73-79 (1991).
19. Khriplovich, I. B., and Lamoreaux, S. K., *CP Violation without Strangeness. The Electric Dipole Moments of Particles, Atoms and Molecules*. Berlin, Heidelberg, New York: Springer-Verlag, 1997.
20. Murthy, S. A., Krause, D. Jr., Li, Z. L., and Hunter, L. R., *Phys. Rev. Lett.* **63**(9), 965-968 (1989).
21. Commins, E. D., Ross, S. B., DeMille, D., Regan, B. C., *Phys. Rev. A* **50**(4), 2360-2377 (1994).